

Nanoscale analysis of the In and N spatial redistributions upon annealing of GaInNAs quantum wells

J.-M. Chauveau, A. Trampert,^{a)} and K. H. Ploog
Paul-Drude Institut für Festkörperelektronik, Hausvogteiplatz 5-7, D-10117 Berlin, Germany

E. Tournié
CEM2, Université de Montpellier II-CNRS, UMR5507, F-34095 Montpellier, France

(Received 8 October 2003; accepted 29 January 2004)

By using transmission electron microscopy on as-grown and annealed GaInNAs/GaAs heterostructures, we demonstrate that annealing induces a correlated behavior of both In and N species within the GaInNAs quantum well. While no intermixing occurs, the analysis of the strain situation reveals that the main driving force for the observed inward diffusion is not composition gradients at the interfaces, but local strain fields. This mechanism leads to the improvement of the photoluminescence (PL) properties and to the blueshift of the PL peak. © 2004 American Institute of Physics. [DOI: 10.1063/1.1690108]

Dilute (Ga,In)(N,As) nitrides have recently received large experimental and theoretical interests because of their particular optical properties¹ and their possible application in GaAs-based long-wavelength optoelectronic devices.² However, the incorporation of N into (Ga,In)As often leads to the deterioration of optical properties,³ along with a degradation of the structural properties (composition fluctuations⁴ or phase separation⁵). Different strategies of post-growth annealing have been demonstrated to improve the photoluminescence (PL) efficiency, yet resulting in an undesirable blueshift of the PL emission.^{6–8} Two distinct mechanisms were proposed as origin of the blueshift. One relies on the diffusion of N out of the (Ga,In)(N,As) quantum well (QW) and/or a Ga/In intermixing at the QW interfaces.^{4,6,7} On the other hand, theoretical studies have shown that the atomic configuration in a compound semiconductor can strongly affect its optical properties.⁹ It has thus been proposed that the blueshift arises from a bonding reorganization within the Ga_{1-x}In_xN_yAs_{1-y} layers.¹⁰ These conclusions were, however, drawn from indirect spectroscopic measurements.

In this letter, we present direct experimental evidence for In and N redistributions in Ga_{1-x}In_xN_yAs_{1-y} QWs upon annealing by using transmission electron microscopy (TEM). We demonstrate that diffusion and local rearrangement happen simultaneously during annealing of Ga_{1-x}In_xN_yAs_{1-y} layers. However, the diffusion process does not tend to homogenize the whole structure (i.e., towards the suppression of the QW) nor induce a phase separation. On the contrary, it results in a homogeneous and nearly ideal composition profile of the QW, maintaining the interface sharpness.

The nominal In_{0.37}Ga_{0.63}N_{0.035}As_{0.965} QWs were grown on (001) GaAs substrates by solid-source molecular-beam epitaxy equipped with an Addon rf plasma source for N. A 29-monolayer (ML)-thick Ga_{1-x}In_xN_yAs_{1-y} QW and 10 ML GaAs barriers were grown at ~420 °C. The remaining GaAs top barrier layer was grown at 580 °C, which affects our as-grown state by a self-annealing process.¹¹ Nevertheless,

we focus here on the changes that occur upon *ex situ* annealing at our optimum conditions for the PL properties.¹² The *ex situ* annealing was therefore carried out in a conventional way under N ambient at 680 °C for 1 h. The PL measurements were performed using the 488 nm line of an Ar laser and a Ge detector. Cross-sectional TEM foils were prepared from the as-grown and annealed samples in both [110] and $[\bar{1}\bar{1}0]$ projections, using mechanical polishing followed by Ar-ion milling. The In and N composition distributions along the growth direction were determined using the contrast analysis of (002) dark-field images combined with high-resolution (HR) TEM, carried out in a JEOL 3010 microscope equipped with a GATAN CCD camera.

Room- and low-temperature PL spectra of the sample before and after annealing are shown in Fig. 1(a). It is obvious that annealing affects the PL as expected for Ga_{1-x}In_xN_yAs_{1-y} QWs: there is a strong enhancement of the radiative efficiency as well as a blueshift of about 30 meV. Note that emission above 1.5 μm (~0.821 eV) is still observed at 300 K. The PL efficiency in this wavelength range is strongly dependent on the structural quality of the layer; the highest efficiency is achieved for a perfect two-dimensional (2D) morphology of the QW.¹³ Figures 1(b) and 1(c) display the comparison between (002) dark-field TEM images of the QWs before and after annealing. The (002) dark-field intensity depends on the difference of the atomic scattering factors of the elements III and V.¹⁴ The diffracted intensity I_{002} is therefore sensitive to the chemical composition of the alloy. In the case of our quaternary system, a possible combination of the In and N content can generate $I_{002}=0$ near the interfaces. The minimum of intensity occurs during the rising of the In content at the interface. This is the origin of the parallel dark lines defining the QWs, as observed in Figs. 1(b) and 1(c). In the lateral direction, the as-grown sample exhibits a rather homogeneous contrast inside the QW [Fig. 1(b)]. In fact, the fluctuations averaged over 100 nm slightly increase in the Ga_{1-x}In_xN_yAs_{1-y} QW (standard deviation of ~8.5%) compared to the GaAs barriers (~6.5%). The absence of strong contrast fluctuations indicates small [In] and [N] variations along the in-plane di-

^{a)}Electronic mail: trampert@pdi-berlin.de

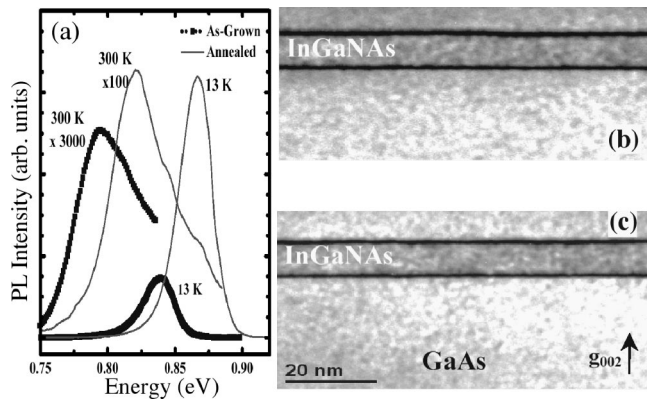


FIG. 1. (a) PL spectra taken from the as-grown (dotted lines) and annealed (solid line) sample at 13 and 300 K. (002) dark-field TEM images of as-grown (b) and annealed (c) QW. The dark lines result from a combination of In and N for which the diffracted intensity is zero. The $\text{Ga}_{1-x}\text{In}_x\text{N}_y\text{As}_{1-y}$ QW is located between these lines. The growth direction is from the bottom to the top of the image.

rection on this scale.^{4,15} Moreover, after annealing, no increase of the contrast fluctuations occurs [Fig. 1(c)], denoting the absence of any phase separation. Additionally, the thickness of the QWs does not fluctuate along the lateral direction, indicating perfect 2D growth with excellent interface quality, with no qualitative changes after annealing. As a consequence, the changes in PL properties are not related to strong structural modifications on a “large scale.”

In order to quantitatively and locally determine the [In] and [N] profiles along the growth direction, a complementary measurement is required.¹⁶ A coherent strain induces displacements of the atomic column positions, related to the tetragonal distortion. The displacements were measured from HRTEM images. Figure 2 displays the local strain calculation from the as-grown sample using the LADIA program package.¹⁷ The strain map confirms straight QW interfaces with a roughness of only a few ML. Moreover, no strong lateral strain variations are detected in this sample, which is consistent with the observations in (002) dark-field. The lat-

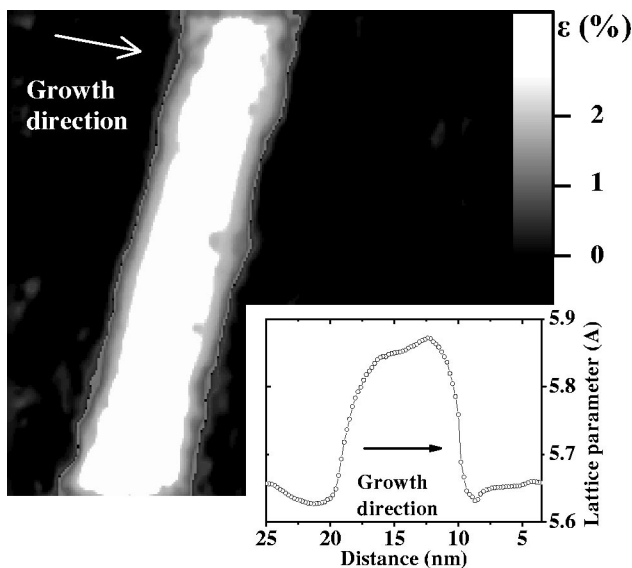


FIG. 2. Vertical strain distribution obtained with the LADIA program package from HRTEM image taken from the as-grown sample. The lattice parameter measured along the growth direction is shown in inset.

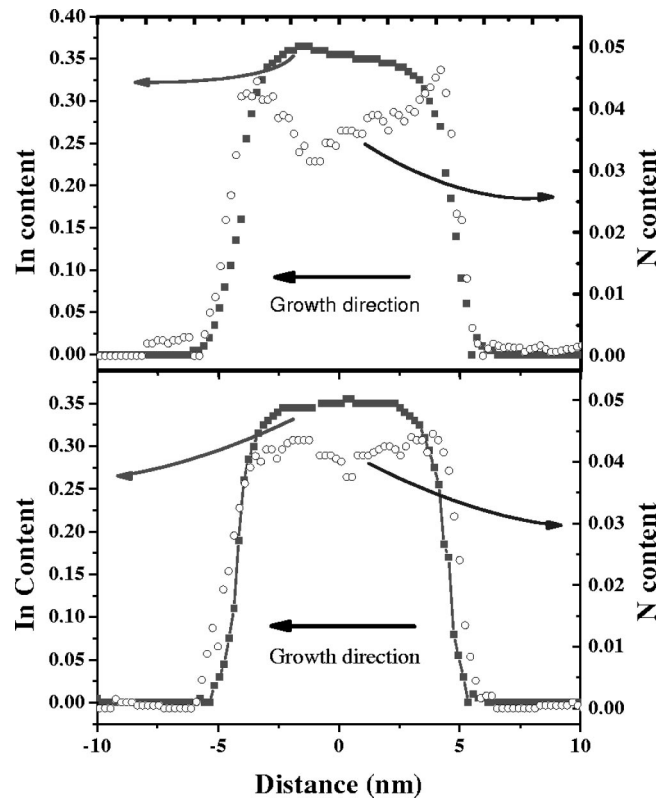


FIG. 3. In and N concentration profiles deduced from the combination of the dark-field intensity and the lattice parameter measurements for the as-grown (a) and annealed (b) QW.

tice parameter in the growth direction (a_{\perp}) was deduced from the analysis of the local displacements and is shown in inset of Fig. 2. In order to increase the accuracy of the measurement, the profile of a_{\perp} was averaged on a lateral length of 20 nm. The combination of the lattice parameter and the dark-field intensity compared to the simulated data gives an unambiguous measurement of In and N content as a function of depth.

Figures 3(a) and 3(b) represent composition profiles of [In] and [N] obtained from the as-grown and the annealed samples, respectively. Before annealing [Fig. 3(a)], the [In] and [N] profiles exhibit an asymmetric and inhomogeneous element distribution in the QW, but with sharp interfaces. The In concentration in the growth direction increases up to 36.5%, while the average value is about 35% inside the QW. This indicates that In surface segregation occurs in $\text{Ga}_{1-x}\text{In}_x\text{N}_y\text{As}_{1-y}$ even at the low growth temperatures used in this work. The [N] profile exhibits a more complex shape with, in particular, a strong increase of the N content at the interfaces (+1.5% compared to the center of the QW). This arises from the growth procedure used for this sample. Indeed, nitrogen can be adsorbed on the surface and subsequently incorporated during the time necessary for stabilizing the N plasma cell at the lower interface, and for switching off the plasma and the N flux at the upper interface. Note that a high amount of N at the interfaces could have a strong influence on the carrier injection due to the existence of nonradiative defects related to N. Annealing clearly leads to the homogenization of the [In] and [N] distributions within the QW in the growth direction, while the QW width is constant (9.5 nm) [Fig. 3(b)]. In addition, the N

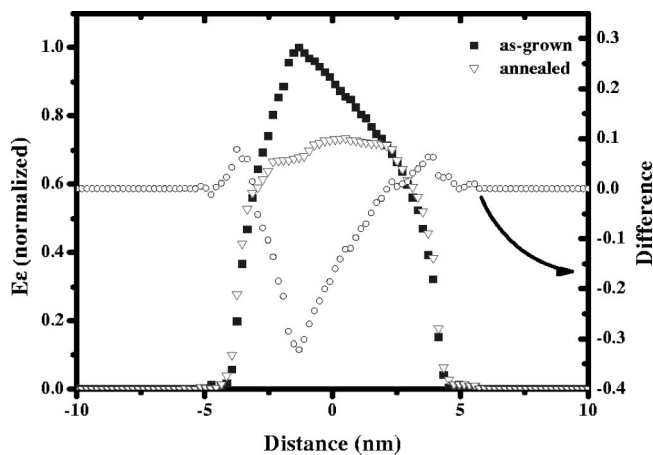


FIG. 4. Elastic strain energies calculated from the profiles. The energy is normalized to the maximum value reached for the as-grown QW. The difference of the strain energy between as-grown and annealed is shown.

concentration at the interface decreases, whereas it increases in the center of the QW from 3.4% to 3.8% after annealing. Moreover, the integrated areas under the [In] and [N] profiles are constant. This confirms *a posteriori* that the sample was homogeneous on a large scale.

Our results thus demonstrate that no interdiffusion of N nor In is detected between the QW and the barrier during annealing, despite the highest gradients of composition at the QW/barrier interface. In contrast, during annealing, both species diffuse inward the QW in order to homogenize the compositions and generate nearly perfect QW profiles. Finally, the In and N displacements are strongly correlated, since In atoms do not diffuse from the QW into the barrier as it does upon annealing N-free GaInAs/GaAs heterostructures.¹⁸ The driving force for this diffusion behavior within the QW may then be related to the reduction of the local strain generated by the large differences in atomic radii between Ga and In, and between As and N.

Furthermore, the reduction of the local strain can affect the total elastic strain state within the QW. Figure 4 shows the calculated average elastic strain energy E_ε before and after annealing as well as the difference of E_ε deduced from the composition profiles. E_ε is a quadratic function of ε [$\varepsilon = (a_{\text{GaAs}} - a_{\text{InGaAs}})/a_{\text{InGaAs}}$] and depends on the thickness and the elastic constants.¹⁹ The $\text{Ga}_{1-x}\text{In}_x\text{N}_y\text{As}_{1-y}$ QW is in a purely pseudomorphic state. We can then consider the QW as a multilayer system with different In and N compositions, each layer having a constant in-plane parameter. E_ε is calculated at every virtual layer. For clarity, E_ε is normalized to the maximum strain energy reached before annealing. The local rearrangement of the N and In atoms within the QW leads to a strong reduction of the total strain energy inside the QW (up to 30%), despite a small increases at the interfaces. Finally, this reorganization within the QW affects the N bonding configuration. Since the N atoms diffuse from interfaces (i.e., Ga-rich area) to an In-rich area in the center, the probability to create an In-rich environment for N atoms is increased. This results in a thermodynamically more stable distribution,¹⁰ which can furthermore be responsible for the blueshift of the PL emission.⁹

It should be pointed out that the diffusion mechanism strongly depends on the initial state of the as-grown sample. Indeed, large compositional fluctuations are related to high defect concentrations²⁰ and the consequential interface roughness is a favorable source for QW intermixing. In this regard, for QWs with lateral fluctuations of $\pm 5\%$ on the In concentration, as observed by Albrecht *et al.*,⁴ the related local strain fluctuations will interfere with the process of N and In diffusion within the QW, and may generate an additional interdiffusion, in contrast to what we observe here. Finally, the observed correlation between [In] and [N] confirms the alloy stability of GaInNAs due to the strong In–N bond.²¹ The diffusion behavior at this temperature depends, thus, on the amount of In and N but also on the [In]/[N] ratio and the local structure.

This work is partially supported by the FET arm of the IST program of the European Commission (project no. IST-2000-26478-GINA1.5). The authors would like to thank Dr. K. Du for making available the LADIA program and his useful comments, and Dr. H. Kim and Dr. M. Ramsteiner for reading of the manuscript.

- ¹M. Weyers, M. Sato, and H. Ando, *Jpn. J. Appl. Phys. Part 2* **31**, L853 (1993).
- ²M. Kondow, T. Kitatani, S. Nakatsuka, M. C. Larson, K. Nakahara, Y. Yazawa, and M. Okai, *IEEE J. Sel. Top. Quantum Electron.* **3**, 719 (1997).
- ³A. Kaschner, T. Lüttger, H. Born, A. Hoffmann, A. Yu. Egorov, and H. Riechert, *Appl. Phys. Lett.* **78**, 1391 (2001).
- ⁴M. Albrecht, V. Grillo, T. Remmele, H. P. Strunk, A. Yu. Egorov, Gh. Dumitras, H. Riechert, A. Kaschner, R. Heitz, and A. Hoffmann, *Appl. Phys. Lett.* **81**, 2719 (2002).
- ⁵R. Asomoza, V. A. Elyukhin, and R. Pena-Sierra, *Appl. Phys. Lett.* **81**, 1785 (2002).
- ⁶Z. Pan, L. H. Li, W. Zhang, Y. W. Lin, R. H. Wu, and W. Ged, *Appl. Phys. Lett.* **77**, 1280 (2000).
- ⁷W. Li, M. Pessa, T. Ahlgren, and J. Decker, *Appl. Phys. Lett.* **79**, 1094 (2001).
- ⁸E. Tournié, M.-A. Pinault, and A. Guzmán, *Appl. Phys. Lett.* **80**, 4148 (2002).
- ⁹K. Kim and A. Zunger, *Phys. Rev. Lett.* **86**, 2609 (2001).
- ¹⁰V. Lordi, V. Gambin, S. Friedrich, T. Funk, T. Takizawa, K. Uno, and J. S. Harris, *Phys. Rev. Lett.* **90**, 145505 (2003).
- ¹¹E.-M. Pavelescu, T. Jouhti, M. Dumitrescu, P. J. Klar, S. Karirinne, Y. Fedorenko, and M. Pessa, *Appl. Phys. Lett.* **83**, 1497 (2003).
- ¹²E. Tournié, M.-A. Pinault, M. Laügt, J.-M. Chauveau, A. Trampert, and K. H. Ploog, *Appl. Phys. Lett.* **82**, 1845 (2003).
- ¹³J.-M. Chauveau, A. Trampert, M.-A. Pinault, E. Tournié, K. Du, and K. H. Ploog, *J. Cryst. Growth* **251**, 383 (2003).
- ¹⁴E. G. Bithell and W. M. Stobbs, *Philos. Mag. A* **60**, 39 (1989).
- ¹⁵A. M. Mintairov, T. H. Kosel, J. L. Merz, P. A. Blagnov, A. S. Vlasov, V. M. Ustinov, and R. E. Cook, *Phys. Rev. Lett.* **87**, 277401 (2001).
- ¹⁶V. Grillo, M. Albrecht, T. Remmele, H. P. Strunk, A. Y. Egorov, and H. Riechert, *J. Appl. Phys.* **90**, 3792 (2001).
- ¹⁷K. Du, Y. Rau, N. Y. Jin-Phillipp, and F. Phillipp, *J. Mater. Sci. Technol.* **18**, 135 (2002).
- ¹⁸S. D. McDougall, O. P. Kowalski, C. J. Hamilton, F. Camacho, B. Qiu, M. Ke, R. M. De La Rue, A. C. Bryce, and J. H. Marsh, *IEEE J. Sel. Top. Quantum Electron.* **4**, 636 (1998).
- ¹⁹J. W. Matthews and A. E. Blakeslee, *J. Cryst. Growth* **27**, 118 (1974).
- ²⁰A. Hierro, J.-M. Ulloa, J.-M. Chauveau, A. Trampert, M.-A. Pinault, E. Tournié, A. Guzmán, J. L. Sánchez-Rojas, and E. Calleja, *J. Appl. Phys.* **94**, 2319 (2003).
- ²¹H. D. Sun, R. Macaluso, S. Calvez, M. D. Dawson, F. Robert, A. C. Bryce, J. H. Marsh, P. Gilet, L. Grenouillet, A. Million, K. B. Nam, J. Y. Lin, and H. X. Jiang, *J. Appl. Phys.* **94**, 7581 (2003).